Discrete element modeling of direct simple shear response of granular soils and model validation using laboratory element tests

Antone Dabeet, Dharma Wijewickreme, & Peter Byrne
University of British Columbia, Vancouver, BC, Canada

2011 Pan-Am CGS Geotechnical Conference

ABSTRACT
The direct simple shear response of spherical granular particles was modeled using discrete element modeling. The modeling approach was validated using a series of laboratory direct simple shear (DSS) element test carried out on air-pluviated glass beads. The results of the model simulations were very similar to those from laboratory testing. The discrete element model also allowed the average lateral stress variations during shear loading to be computed. An overall increase in lateral stress with the progression of shearing was observed in this regard. The noted good agreement of the shear response between numerical modeling and experiments highlights the potential of discrete element modeling to effectively capture the behavior of granular materials.

RÉSUMÉ

La réponse au cisaillement simple direct (CSD) de la masse granuleuse sphérique a été modélisée en utilisant la méthode des éléments discret. L'approche de la modélisation a été validée à partir d'une série d'essai au laboratoire de CSD effectué sur des billes de verres la méthode pluviale dans l'air. En général, les résultats des simulations ont été très proches de celles effectuées en laboratoire. Le éléments discret modèle a permis de calculer les variations moyennes des contraintes latérales pendant l'effort de cisaillement. Nous avons constaté une augmentation globale de la force latérale avec la progression de l'effort de cisaillement. Le bon accord entre la modélisation numérique et les expériences à la réponse au cisaillement souligne le potentiel de la modélisation par éléments discrets pour cerner le comportement des matériaux granuleux.

1 INTRODUCTION

The direct simple shear (DSS) test has been widely used to assess the earthquake response of soils (Bjerrum and Landva 1966; Wood and Budhu 1980; Finn et al. 1982; Wijewickreme et al. 2005). The key reasons for the growing interest in the DSS test has been due to its simplicity and its ability to more realistically simulate field stress conditions that involve rotation of principal stresses.

Continuum-based models are often the preferred approach to simulate DSS behavior of soils (Byrne et al., 2004; Prevost and Hoeg, 1976). As noted by Cundall and Strack (1979), with the recent advances in computers, it is now possible to model soil as discrete particles using the discrete element method (DEM). In DEM, constitutive behavior at the contacts between individual grains is specified. The constitutive model at the contacts level together with Newton's laws of motion are used to compute the macro level behavior of a specimen comprised of granular particles .

One of the advantages of DEM modeling over continuum modeling is the smaller number of input parameters. Previous studies that utilize the DEM provided qualitative predictions only. This study presents a qualitative and a quantitative validation for a DSS model in PFC^{3D} 3.1 (particle flow code in three dimensions based on the DEM by Itasca 2005a). Input parameters for the developed DSS-PFC^{3D} model were obtained through a one to one comparison of the results of monotonic DSS laboratory tests on glass beads and the results of the DSS-PFC^{3D} simulations. Currently, there are no established guidelines for the selection of interparticle contact stiffness/friction parameters for PFC^{3D} models. Therefore, it was required to conduct parametric analysis to obtain the parameters that would best simulate the observed experimental behavior.

The paper is organized into four parts. A brief description of PFC^{3D} is presented in Section 2 followed by the results of monotonic drained DSS laboratory tests on 2-mm diameter glass beads presented in Section 3. Results of monotonic drained simulations using the DSS-PFC^{3D} model are presented in Section 4.

2 OVERVIEW ON PFC^{3D}

Particle Flow Code in three dimensions (PFC^{3D}) is based on the discrete elements method by Cundall and Strack (1979) and Itasca (2005a). Soil particles are modeled as rigid spheres (referred to as balls). The contacts between balls are modeled using the soft contacts approach that allows particle to virtually overlap (Itasca, 2005b). The magnitude of the overlap is related to the forces at the contacts by normal and shear stiffness values, K_n and K_s, respectively. These stiffness values have the units of force/displacement. In this paper, identical values were used for normal and shear stiffness parameters. Accordingly, a single interparticle stiffness parameter, K, was used to refer to both K_n and K_s.

Maximum friction at the contacts can be specified. Slippage occurs if the ratio of shear to normal forces exceeds maximum friction, F. Boundaries are referred to as walls. The contacts between the balls and walls are modeled in a similar way to contacts between balls. The code uses an explicit solution scheme.

The discrete element method and PFC in particular have been increasingly used in modeling soils (Cheng et al. 2003; Powrie et al. 2005; Pinheiro et al. 2008; Dabeet et al. 2010).

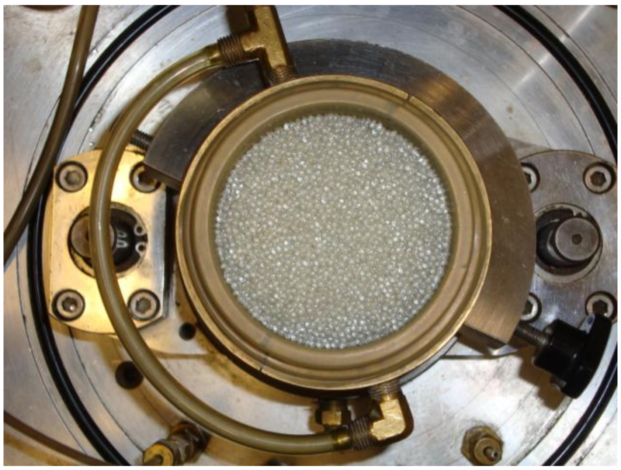

Figure 1. 2mm air pluviated glass beads in the DSS cylindrical cavity at the end of specimen preparation.

Table 1. Summary of consolidation void ratio values obtained during consolidation of monotonic DSS test specimens of air-pluviated 2 mm diameter glass beads.

Lab test ID	e_c	σ'_{zzc} (kPa)
GLS-2mm-100-D-M	0.6	100.7
GLS-2mm-100-D-M-R	0.606	100.6
GLS-2mm-150-D-M	0.598	151
GLS-2mm-200-D-M	0.593	200.4

3 LABORATORY TESTING PROGRAM

3.1 Material tested and specimen preparation method

Uniform spherical glass beads, 2-mm average diameter, were used as the test material. The test specimens were prepared using the method of air-pluviation. The glass beads were rained into the specimen mold of the DSS device under gravity using a funnel with a bottom opening having a diameter equal to 1 cm. The raining was performed so that the particles had a drop height of 17 cm above the top of the specimen. The final surface of the specimen was obtained by traversing a suction tube connected to a vacuum supply of about 30 kPa. The vacuum process allowed the removal of excess particles and produced a final levelled surface with minimum disturbance to the particles below the top surface of the specimen. A photograph showing the specimen of glass beads at the end of specimen preparation is presented in Figure 1.

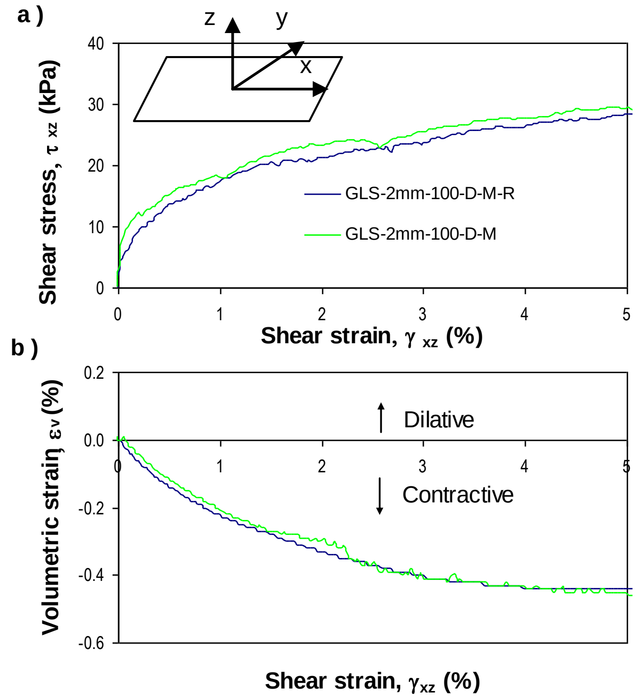

Figure 2. Results of DSS tests GLS-2mm-100-D-M and GLS-2mm-100-D-M a) Shear stress strain response b) volumetric strain vs. shear strain.

3.2 Test program

The NGI-type DSS device at the University of British Columbia (UBC) was used as the test apparatus for monotonic shear testing (Bjerrum and Landva, 1966). The UBC-DSS device allows the testing of a soil specimen having a diameter of around 70 mm and height of 20–25 mm. In the DSS device, the specimen diameter is constrained laterally using a steel-wire reinforced rubber membrane.

Four drained monotonic DSS tests were performed (see Table 1). Tests GLS-2mm-100-D-M and GLS-2mm-100-D-M-R were performed under identical conditions, and these tests served to demonstrate the repeatability of the testing method. As noted in Table 1, two other drained monotonic shear tests were conducted with specimens initially consolidated to different initial vertical effective consolidation stresses of 100 kPa, 150 kPa, and 200 kPa. In addition to providing the characteristic drained shear response, the tests allowed an opportunity to examine effect of vertical effective stress on the drained monotonic shear behavior of glass beads.

3.3 Test results

Void ratios and vertical effective stress of the tested specimens at the end of consolidation are shown in Table 1. The change in void ratio due to increase in the vertical effective stress, σ'_{zz}, is very small for the tested stress range.

The shear behavior for essentially identical tests GLS-2mm-100-D-M and GLS-2mm-100-D-M-R are presented in Figure 2. As may be noted, except for the slightly stiffer response noted for GLS-2mm-D-M, the two specimens displayed very similar shear stress strain characteristics and, thereby, confirming the repeatability of the specimen preparation method as well as the testing method.

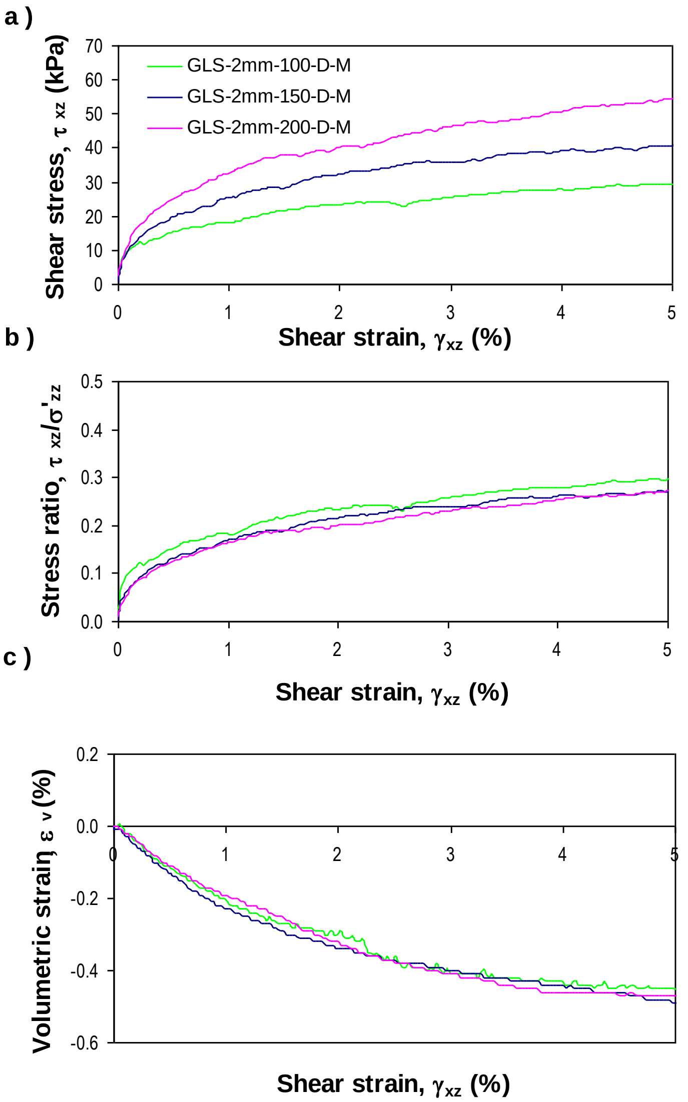

Figure 3. Results of DSS tests GLS-2mm-100-D-M, GLS-2mm-150-D-M, and GLS-2mm-200-D-M a) Shear stress strain response b) Stress ratio shear strain response c) volumetric strain vs. shear strain.

The results obtained from the tests GLS-2mm-100-D-M, GLS-2mm-150-D-M and GLS-2mm-200-D-M are superimposed in Figure 3. As expected, the shear resistance, τ_{xz}, increased with increasing vertical (normal) effective consolidation stress σ'_{zz}. When the results are plotted in terms of stress ratio vs. Shear strain (γ_{xz}), the curves for the three tests essentially overlap as shown in Figure 3b.This observation is in accord with typically observed behavior for granular materials such as Fraser River sand.

The three tests show similar shear induced contractive response with the development of shear strain (Figure 3c). It is known that, during shear loading in general, the contractiveness of soil increases with increasing effective confining stress. It appears that the effect of stress densification (i.e. increase in density due to the increase in stress level) counters the shear induced contractiveness with the increase in stress level; similar observations have been made by Wijewickreme et al. (2005) during cyclic loading tests on Fraser River sand. The net result is volumetric strain versus shear strain response that is relatively insensitive to the change in vertical effective stress within the range of investigated σ'_{zz} values.

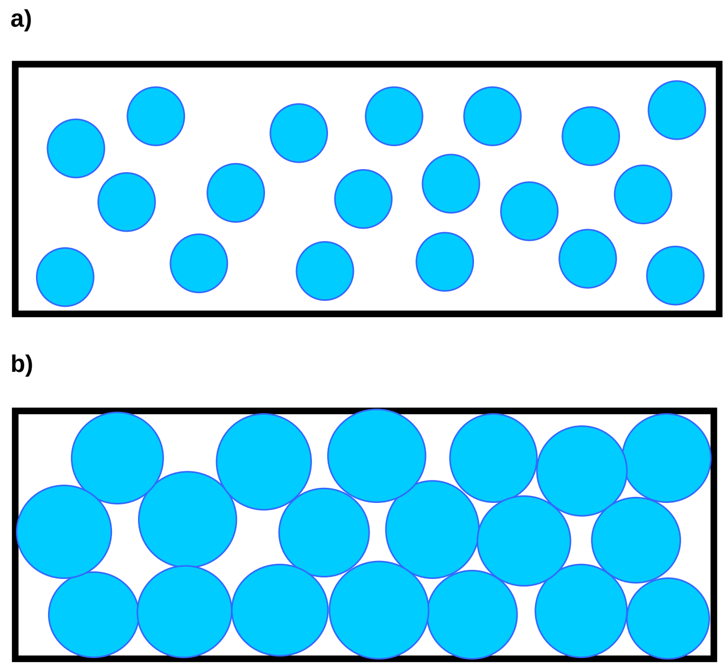

Figure 4. Schematic illustrating sample preparation by particle expansion. a) after particle generation and before particle expansion; and b) after particle expansion.

4 DISCRETE ELEMENT SIMULATIONS

4.1 Analysis methodology

A DSS specimen with a height of 2 cm and a diameter of 7 cm filled with “balls” was considered for the PFC simulation herein, leading to a height to diameter ratio of around 0.3. These specimen dimensions selected for the DEM analysis are very similar to the real or physical DSS specimen dimensions used for the glass beads testing discussed in the previous section.

Table 2. Parameters used for PFC^{3D} simulations of monotonic DSS testing

Simulation ID	Interparticle stiffness parameter - K (kN/m)	F	σ'_{zzc} (kPa)	e_c	k_o ($\sigma'_{xxc}/\sigma'_{zzc}$)
K5e5-F0.2-100-D-M	500	0.2	101.9	0.614	0.73
K5e5-F0.2-150-D-M	500	0.2	149.3	0.612	0.7
K5e5-F0.2-200-D-M	500	0.2	197	0.61	0.68
K5e4-F0.2-100-D-M	50	0.2	100.4	0.596	0.68
K5e4-F0.2-150-D-M	50	0.2	149.3	0.576	0.68
K5e4-F0.2-200-D-M	50	0.2	199	0.553	0.74
K5e4-F0.25-100-D-M	50	0.25	98.7	0.601	0.69
K5e4-F0.3-100-D-M	50	0.3	100.3	0.602	0.67

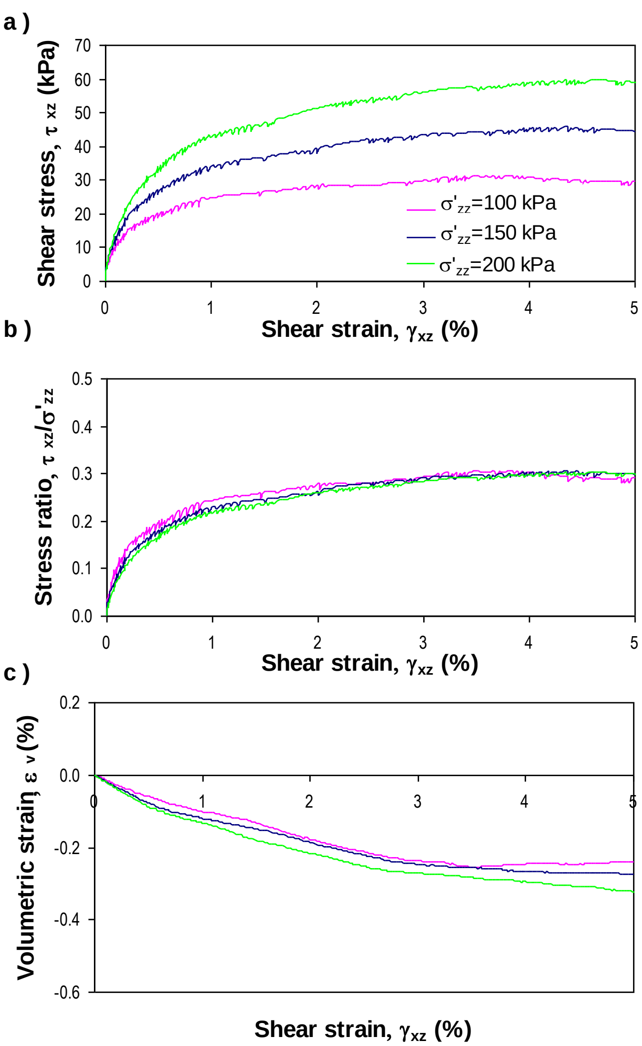

Figure 5. Shear response from DSS-PFC^{3D} model for K = 500 kN/m and F = 0.2 for σ'_{zz} values of 100kPa, 150kPa, and 200kPa: a) Shear stress strain response; b) Stress ratio shear strain response; c) volumetric strain vs. shear strain.

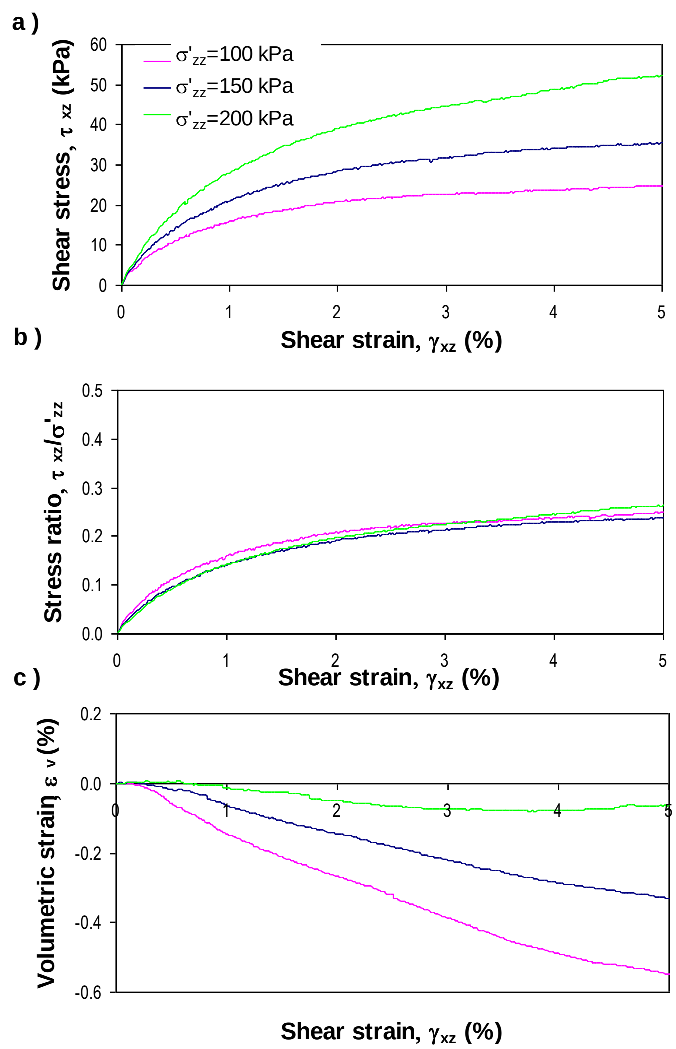

Figure 6. Shear response from DSS-PFC^{3D} model for K = 50 kN/m and F=0.2 for σ'_{zz} values of 100 kPa, 150 kPa, and 200 kPa: a) Shear stress strain response; b) Stress ratio shear strain response; and c) volumetric strain vs. shear strain.

In the simulations reported in this paper, the balls were first randomly generated inside the specimen cavity with an initial ball diameter smaller than their intended final diameter. The diameter of the balls was then increased to the final diameter for the analysis and contacts are formed. The particles assembly formation is illustrated in Figure 4. Figure 4a shows the generated balls with an initial diameter smaller than their intended final diameter. The final assembly is shown in Figure 4b after particle expansion (i.e. increase in particles diameter). The final assembly of balls has uniform particles with a diameter of 2 mm, which is identical to that of the tested glass beads. The number of generated balls to fill the specimen size is around 10,000.

In the PFC model, the specimen is bounded by a top cap, a bottom cap, and a cylindrical wall that provides lateral support. A rigid cylindrical wall is modeled. It provides uniform boundary shear strain, γ_{xz}, during the shearing phase.

The specimen was consolidated by moving the top and bottom boundaries simultaneously at a rate of 2 mm/second. The time step was set to around 10^{-6} seconds for each computation cycle (i.e. it takes one million computation cycles to displace each of the walls by 2 mm). The numerical processing time depends on the number of balls in the model and on the computation power available.

The Measurement Sphere (MS) routine in PFC^{3D} is used to calculate local stresses and porosities. The MS routine computes the stress tensor from forces at contacts averaged over the volume of the selected MS. Stresses and void ratios reported in the following sections are calculated at the specimen core using a central measurement sphere with a radius of 0.8 cm.

The specimen shearing is modeled by rotating the cylindrical lateral boundary around the Y-axis shown in Figure 2a. Top and bottom boundaries are simultaneously displaced horizontally as a function of shear strain in the positive and negative x-directions, respectively. They are allowed to move in the z-direction during drained shearing to maintain the desired σ'_{zz}.

The boundary shear strain rate used was 2.5 rad/s with a fixed time step of 0.5 x 10^{-6} seconds /computation cycle. For drained shearing, the vertical stress subroutine is called to correct σ'_{zz} to its pre-shearing value to a tolerance of ±0.5 kPa. This is performed by moving the upper and lower boundaries simultaneously.

4.2 Input parameters for numerical simulation

A series of DEM simulations were undertaken to model monotonic DSS loading of specimens developed using balls as summarized in Table 2. For the convenience of recognition, the numbering format used for identifying the computer simulations were purposely chosen to closely match with the stress conditions of the DSS tests that were simulated. As noted earlier, in the absence of established guidelines, it was necessary to conduct parametric analysis for interparticle contact stiffness and, in turn, appropriately simulate the observed experimental behavior as presented in the previous section. The interparticle stiffness parameter (K) values of 50 kN/m and 500 kN/m were used to model the ball-ball and ball-wall contacts, respectively. The stiffness parameter at contacts controls the amount of compressibility of the simulated assembly of particles. Accordingly, the assembly with the relatively lower stiffness is expected to demonstrate relatively more compression in response to a given increase in stress level.

The simulated specimens were consolidated using ball-ball friction (F) values of 0.2, 0.25, and 0.3, and a zero ball-wall friction to minimize shear stresses generated during consolidation. During shearing, the top and bottom wall-ball friction coefficient is given a high value of 10 for all simulations to minimize slippage at the top and bottom platens of the simple shear test. Frictionless contacts at the lateral cylindrical wall were assumed for all other simulations. This is similar to the low friction contact at the reinforced membrane for the real DSS specimen. The effect of vertical effective stress was investigated for the three values of 100 kPa, 150 kPa, and 200 kPa. All simulations were conducted assuming drained conditions. Specific gravity of 2.67 was specified for the balls. Viscous damping was used with a damping ratio of 0.7.

4.3 Results of DEM Simulation

The simulations K5e5-F0.2-100-D-M, K5e5-F0.2-150-D-M, and K5e5-F0.2-200-D-M resulted in end-of-consolidation void ratios of 0.614, 0.612, 0.61, respectively (Table 2). This means that the effect of vertical effective stress level on the void ratio at the end of consolidation for the simulation cases with K = 500 kN/m is marginal. The simulations K5e4-F0.2-100-D-M, K5e4-F0.2-150-D-M, and K5e4-F0.2-200-D-M where the value of K was kept at 50 kN/m (i.e., ten times lower stiffness than the above) was seen to result in softer contacts and the effect of vertical effective stress level on the void ratio at the end of consolidation was relatively more significant. The effect of stress densification (i.e. decrease in void ratio due to increase in stress level) on the shearing behavior of the simulated DSS specimen will be shown later in this section.

As per above, the stiffness parameter K clearly has a significant control over the void ratio at the end of consolidation. Simulations K5e4-F0.2-100-D-M, K5e4-F0.25-100-D-M, and K5e4-F0.3-100-D-M with varying F values have shown that, although the effect is marginal, higher F values would result in slightly higher end-of-consolidation void ratio values (see Table 2). This may be due to the less potential for slippage at the contacts with increased F values.

In the most commonly used version of the DSS test, lateral stress acting on the vertical plane is usually not measured. On the other hand, the DSS-PFC^{3D} numerical model would allow computing the lateral stress using forces at particle contacts on the vertical wall. Accordingly, a lateral stress coefficient, k, at the end of consolidation of around 0.7 was computed for the simulations presented in Table 2. A trend of decreasing lateral stress coefficient with the increase in vertical effective stress level was observed for the simulations with interparticle stiffness parameter (K) = 500 kN/m. However, this trend was not observed for the simulations with K = 50 kN/m.

The effect of vertical effective stress on the shear stress, τ_{xz}, shear strain, γ_{xz}, response for the simulations with K of 500 kN/m is shown in Figure 5a. As expected, the simulation with σ'_{zz} of 200 kPa has the highest shear stresses followed by the simulations with σ'_{zz} of 150 kPa, and 100 kPa. As typically observed for granular materials, stress ratio, τ_{xz} / σ'_{zz}, with the development of shear strain is not affected by the change in the vertical effective stress level (see Figure 5b). During shearing, as shown in Figure 5c, the three simulated specimens demonstrated similar contractive volumetric strains with the simulation for σ'_{zz} = 200 kPa showing slightly more contractive volumetric strains. Typically, granular materials would develop more shear-induced contraction at higher stress levels. The K = 500 kN/m simulations displayed only marginal difference in shear induced contractiveness for the investigated stress level range. It may be possible that the slight increase in dilatancy due to stress densification effect (i.e., slightly lower voids ratio arising due to consolidation) would have reduced the contractive tendency associated with increased confining stress level.

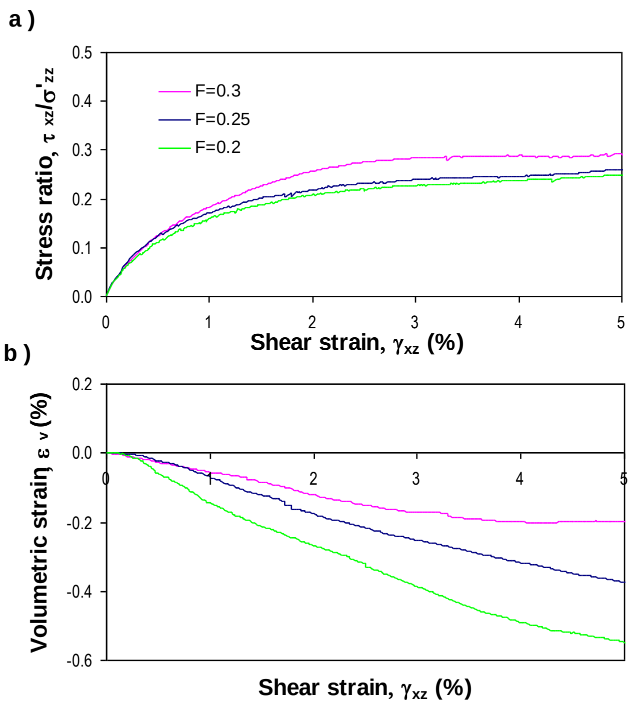

Figure 7. Shear response from DSS-PFC^{3D} model for K = 50 kN/m and F values of 0.2, 0.25, and 0.3: a) Stress ratio shear strain response; and b) volumetric strain versus shear strain.

Similarly, the effect of vertical effective stress level on the shearing response was investigated for K of 50 kN/m as shown in Figure 6 (i.e., simulations K5e4-F0.2-100-D-M, K5e4-F0.2-150-D-M, and K5e4-F0.2-200-D-M). The shear stress strain plot showed a softer response compared to that for the simulations with K = 500 kN/m in Figure 5a. As may be noted from Figure 6b, the three simulations resulted in an essentially identical stress ratio versus shear strain response. Contrary to the observations for the simulations with K of 500 kN/m, volumetric strain response for the simulations with K = 50 kN/m were significantly sensitive to changes in vertical effective stress level (see Figure 6c). In essence, simulation K5e4-F0.2-100-D-M that had the largest end-of-consolidation void ratio developed the greatest amount of shear-induced contractive volumetric strain, with decreasing levels of contractive volume changes for the simulations K5e4-F0.2-150-D-M and K5e4-F0.2-200-D-M. Clearly, the use of a relatively low K = 50 kN/m does not seem to be suitable for modeling the laboratory observed direct simple shear response of glass beads.

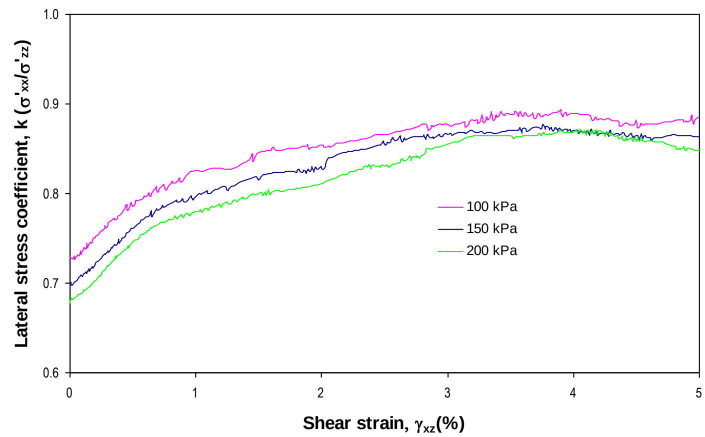

Figure 8. Variation in coefficient of lateral stress with the development of shear strain for DSS tests simulated with σ'_{zz} values of 100 kPa, 150 kPa, and 200 kPa (for K = 500 kN/m and F = 0.2).

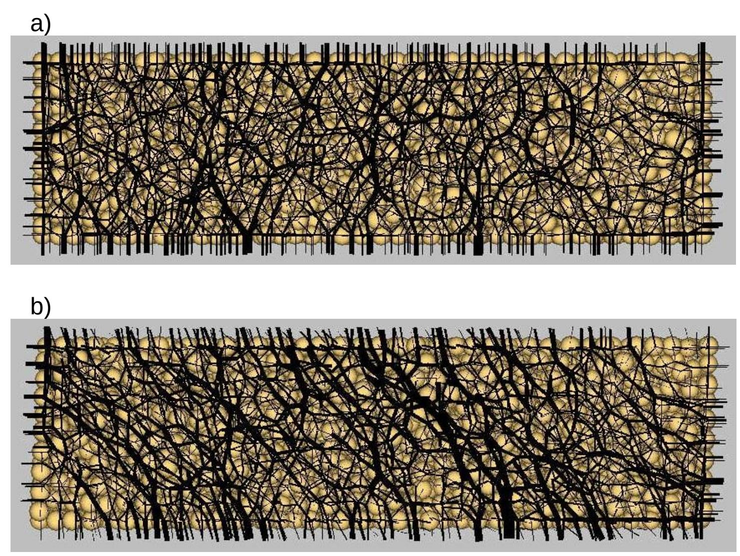

Figure 9. A central cross section through the simulated DSS specimen parallel to the x-axis showing contact forces: a) at the end of consolidation and prior to shearing; and b) at 4% shear strain.

The effect of the friction parameter on the shear stress strain response was investigated for simulations with K = 50 kN/m for F values of 0.2, 0.25, and 0.3 (see Figure 7). The peak mobilized stress ratio was observed to generally increase with increasing value of F as shown in Figure 7a (although the simulation with F = 0.25 was only slightly higher than that for the case with F = 0.2). Less friction at particle contacts seem to have increased the potential for slippage, and, in turn, resulting in a more contractive behavior (Figure 7b)

The knowledge of lateral stresses during shearing is an important consideration in the interpretation of DSS data to obtain soil parameters. The results of the DSS test simulations indicated that the coefficient of lateral stress increased with the development of shear strain. The coefficients of lateral stress for simulations K5e5-F0.2-100-D-M, K5e5-F0.2-150-D-M, and K5e5-F0.2-200-D-M are shown in Figure 8. The coefficient of lateral stress increases from an initial value of around 0.7 to a value of around 0.9 at 5% shear strain. This trend is in agreement with observations by Budhu (1985) from DSS tests on Leighton Buzzard sand.

Another advantage of discrete elements modeling using PFC^{3D} is that forces at the contacts (called "force chains") can be viewed graphically at any stage of the simulation. Contact forces for simulation K5e5-F0.2-100-D-C4% are shown in Figure 9 (a) and (b) as black lines at shear strains of 0% and 4%, respectively. The thickness of the black lines is proportional to the magnitude of contact forces. At 0% shear strain, a significant number of strong force chains can be seen to be aligned generally in the vertical direction (Figure 9a) which is the direction of major principal stress after consolidation and before shear. However, at 4% shear strain as can be seen in Figure 9b, most of the strong force chains are oriented in a direction that is inclined to the vertical direction. This is expected because with a shear stress applied on the specimen, the major principal stress will rotate and be inclined. The strong force chains will therefore rotate and be inclined in a direction consistent with the rotation of the direction of major principle stress.

5 DISCUSSION AND CONCLUSIONS

The research findings presented herein demonstrate that discrete element modeling has the ability to capture some of the salient mechanical response observed during laboratory direct simple shear (DSS) testing of spherical glass beads. These include the ability of the DEM to capture: (i) the observed contractive shear induced volumetric strain response; (ii) reduction of the degree of shear-induced contractiveness due to increase in confining stress level as a result of stress densification; (iii) unique normalized shear stress versus shear strain response for DSS tests conducted at different vertical effective stress levels; (iv) expected increase in lateral stress with development of shear strain; (v) the rotation of the direction of major principle stress anticipated in DSS loading.

The performed parametric study showed that the use of a relatively high interparticle stiffness parameter (K) of 500 kN/m yields shear stress strain and volumetric strain responses that are more similar to these observed from experimental data (compared to the case of particles with K = 50 kN/m). The selection of suitable input parameters appears to be one of the key challenges in simulating the interaction between particles during shear loading.

In an overall sense, the agreement of the results of the DSS-PFC^{3D} model with the experimental data presented in this paper, supports the observations in literature that discrete elements modeling has a strong potential to simulate the behavior of granular materials.

REFERENCES

Bjerrum, L., and Landva, A. 1966. Direct simple shear tests on a Norwegian quick clay. *Geotechnique*, 16:1-20

Budhu, M. 1985. Lateral stesses observed in two simple shear apparatus. Journal of Geotechnical Engineering, 111: 698-711.

Byrne, P.M, Park, S., Beaty, M., Sharp, M., Gonzalez, L., Abdoun, T. 2004. Numerical modeling of liquefaction and comparison with centrifuge tests. *Canadian Geotechnical Journal*, 41: 193-211.

Cheng, Y.P., Nakata, Y., and Bolton, M.D. 2003. Discrete element simulation of crushable soil. *Geotechnique*, 53: 633-641.

Cundall, P.A., and Strack, O.D.L. 1979. A discrete numerical model for granular assemblies. *Geotechnique*, 29: 47-65.

Dabeet, A., Wijewickreme, D., and Byrne, P. 2010. Evaluation of the stress-strain uniformities in the direct simple shear device using 3D discrete element modeling. *Canadian Geotechnical Conference*, Calgary.

Finn, W.D.L., Bhatia, S.K., and Pickering D.J. 1982. The cyclic simple shear test. In *Soil Mechanics- Transient and Cyclic Loads*. John Wiley & Sons Ltd., 583-607.

Itasca Consulting Group, Inc. 2005a. PFC^{3D} (Particle Flow Code in Three Dimensions), Version 3.1. Minneapolis, USA.

Itasca Consulting Group, Inc. 2005b. PFC^{3D} user manual. Minneapolis, USA.

Pinheiro, M., Wan, R., and Li, Q. 2008. Drained-undrained response and other fundamental aspects of granular materials using DEM. *Canadian Geotechnical Conference*, Edmonton: 224-231.

Powrie, W., Ni, Q., Harkness, R., and Zhang, X. 2005. Numerical modeling of plane strain tests on sands using a particulate approach. *Geotechnique*, 55: 297-306.

Prevost, J., Hoeg, K. 1976. Reanalysis of simple shear soil testing. *Canadian Geotechnical Journal*, 13: 418-429.

Roscoe, K., Bassett, R., Cole, R. 1967. Principal axes observed during simple shear of sand. *Proceedings of the Geotechnical Conference on Shear Strength Properties of Natural Soils and Rocks,* Oslo: 231-237.

Wijewickreme, D., Sriskandakumar, S., and Byrne, P.M. 2005.Cyclic loading response of loose air-pluviated Fraser River Sand for validation of numerical models simulating centrifuge tests. *Canadian Geotechnical Journal*, 42: 550-561.

Wood D.M., and Budhu, M. 1980. The behaviour of Leighton Buzzard Sand in cyclic simple shear tests. *International Symposium on Soils under Cyclic and Transient Loading*, A. A. Balkema, Rotterdam: 9-21.